Ecotoxicology and Environmental Safety 219 (2021) 112305

Contents lists available at ScienceDirect

Ecotoxicology and Environmental Safety

journal homepage: www.elsevier.com/locate/ecoenv

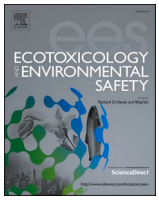

Toxic effects of Decabromodiphenyl ether (BDE-209) on thyroid of broiler chicks by transcriptome profile analysis

Lin Cheng, Junhua Yang, Qinxiong Rao, Zehui Liu, Wei Song, Shuhui Guan, Zhihui Zhao *, Weiguo Song *

Institute for Agri-food Standards and Testing Technology, Shanghai Academy of Agricultural Science, Shanghai 201106, China

ARTICLE INFO

Edited by: Dr. Caterina Faggio

Keywords:
Broiler chicks
Decabromodiphenyl ether
Histopathology
Thyroid hormones
Transcriptome analysis

ABSTRACT

The wide usage of decabromodiphenyl ether (BDE-209) results in its increasing occurrence in the environment and increasing attention in regard to human and animal health. BDE-209 is an endocrine disruptor for hypothyroidism, but the toxicity mechanism is unclear. Here, the histopathology and transcriptome sequencing of thyroid tissue from broiler chicks were investigated by supplemental feeding with different concentrations of BDE-209 for 42 days (0–4 g/kg in basal diet), followed by determining the levels of thyroid hormones in serum. The results showed ruptured and even hyperplastic follicular epithelial cells in the thyroid, and a total of 501 differentially expressed genes were screened out: 222 upregulated and 279 downregulated. Based on the Kyoto Encyclopedia of Genes and Genomes database, neuroactive ligand-receptor interaction pathway was significantly enriched, and α1D-adrenergic receptor, follicle-stimulating hormone receptor, thyroid stimulating hormone receptor, and somatostatin receptor type 2 were shown to be candidate biomarkers. Thyroxine was a possible biomarker due to clear reduction in serum and significant correlation with exposure concentrations. These results suggested that oral intake of BDE-209 can cause structural injuries and even hyperplasia, and affect gene transcription involved in the neuroactive ligand-receptor interaction pathway of thyroid, as well as thyroid hormones in serum.

1. Introduction

Decabromodiphenyl ether (BDE-209) is the predominant constituent of commercial deca-BDE mixtures, and has been widely used for more than four decades to improve fire resistance of a multitude of products, such as furniture, textiles, and building materials (Rahman et al., 2001; Wilford et al., 2005). Despite the characteristics of bioaccumulation, long-range transportation, and biological toxicity (Covaci et al., 2011), BDE-209 is still produced and consumed in China and many other developing countries in Asia (Yu et al., 2016). Currently, BDE-209 is reported to be widely distributed in air, dust, sediment, water, fish, birds, and even in human samples such as hair, breast milk, blood, and feces (Qiao et al., 2018). Meanwhile, as the most abundant BDE congener, BDE-209 can bioaccumulate and biomagnify through both aquatic and terrestrial food webs (Chen et al., 2008).

There is ongoing human exposure to BDE-209 from diet and dust in indoor environments (Zhu et al., 2015). In animal-derived food, like chicken muscle and liver tissues, duck meat, eggs, and fishmeal (Luo et al., 2009; Labunska et al., 2013; Li et al., 2018), BDE-209 is the dominant component among all BDE congeners, and its adverse effects on organisms have attracted much attention. BDE-209 has been reported to be an endocrine disruptor, such as in hypothyroidism (Darnerud, 2008), and could interfere with adult human thyroid hormone levels (Turyk et al., 2008). The possible mechanisms include competitive binding to the thyroid transport protein transthyretin and thyroid hormone receptors (Richardson et al., 2008), and affecting thyroxine (T4) metabolism because of structural similarity to thyroid hormones (Chen et al., 2018). In rats, BDE-209 exposure can disturb the blood levels of T4 or triiodothyronine (T3) (Kim et al., 2009). However, the mechanism of BDE-209 action on the thyroid remains unclear.

Given the exposure risk of BDE-209 to animals, we aimed to examined the toxic effects of BDE-209 on thyroid of broiler chicks, which is an important economic species of livestock animals, by supplementing different amounts of BDE-209 into their daily diet. Here, histopathological observation of thyroid tissue from broiler chicks was performed after diet exposure for 42 days. Because transcriptome sequencing

* Corresponding authors.
E-mail addresses: 18918162068@163.com (Z. Zhao), songweiguo@saas.sh.cn (W. Song).

https://doi.org/10.1016/j.ecoenv.2021.112305
Received 3 February 2021; Received in revised form 28 April 2021; Accepted 30 April 2021
Available online 21 May 2021
0147-6513/© 2021 Published by Elsevier Inc. This is an open access article under the CC BY-NC-ND license (http://creativecommons.org/licenses/by-nc-nd/4.0/).

(RNA-Seq) can quantify a large dynamic range of expression levels with absolute values derived from read alignments (Sabino et al., 2018), RNA-Seq analysis was carried out to illustrate the transcriptome profile of the thyroid and to screen out potential genes and pathways involved in the response to BDE-209, following by quantitative real-time PCR (QRT-PCR) quantification. In addition, the levels of thyroid hormones in serum were determined to further explore the toxic effect of BDE-209 on the downstream hormone regulation of the thyroid. These results would be helpful to our understanding of the mechanisms of endocrine-toxic induced by BDE-209.

2. Materials and methods

2.1. Experimental design and management

A total of 150 1-day-old healthy male broilers (Arbor Acres) with an average body weight of 50.25 ± 0.26 g were randomly allotted to five experimental groups: control (basal diet, n = 30), 0.004 g/kg (basal diet with 0.004 g/kg BDE-209, n = 30), 0.04 g/kg (basal diet with 0.04 g/kg BDE-209, n = 30), 0.4 g/kg (basal diet with 0.4 g/kg BDE-209, n = 30), and 4 g/kg (basal diet with 4 g/kg BDE-209, n = 30). The basal diet was obtained from Jiangsu Guangda Livestock and Poultry Co. Ltd (Changzhou, China), and the composition is shown in Table S1. The BDE-209 (> 98% purity) was purchased from Shanghai Macklin Biochemical Co., Ltd (Shanghai, China). The whole experiment period was 42 days with continuous exposure. All diets were formulated to meet or exceed the nutritional requirements of broiler chicks (1994) (Woyengo et al., 2018).

At 1 d of age, 10 birds of each group were transferred into a cage, and each group had 3 cages. When growing for four weeks, the 30 broilers in each group were placed in 6 electrically heated cages randomly, and each cage included 5 broilers During the trial period, the temperature was set at 35 °C in the first week followed by a 3 °C/week of reduction until five weeks, and the relative humidity was kept at 40–50%. Meanwhile, a 24 h lighting was set in the first three days, then "23-hour-on-1-hour-off" during 4 weeks, and a "5-hour-on-1-hour-off, 4 cycles" lighting for 5–6 weeks (Sun et al., 2021). Each cage was equipped with an external feeding trough and four built-in water cups. The fresh feed was provided daily at 8:00 am with ad libitum feeding. Further, the concentrations of PBDEs in broilers feed were detected by gas chromatography/high-resolution mass spectrometry (Thermo Fisher Scientific Inc. CN, Shanghai, China) before the experiment to ensure the total concentration of BDE-209 (< 0.12 ng/g) (Sun et al., 2021; Li et al., 2018). During the trial period, body weight and intake of all birds was recorded every week, and any clinical signs and deaths were recorded. The birth weight, terminal weight, average daily gain, average daily consumption charge, and feed/gain of broilers in each group were record in Table S2.

All procedures on experimental animals were carried out in accordance with the Guidelines of Animal Ethics Committee in Shanghai Academy of Agricultural Sciences (Approval Number: SAASPZ0920001). In addition, significant effort was conducted to improve the general well-being of chicks, and once any sign of illness was observed during rearing or sampling procedures, the chicks were excluded from the experiment and given veterinary care according to the Guidelines of Animal Ethics Committee.

2.2. Sample collection

After feeding for 42 days, the body weight of 30 chicks in each group was measured. Then, blood samples were obtained from the wing veins of all birds and centrifuged at 700 g for 15 min at room temperature by using Tabletop Refrigerated Centrifuge (Eppendorf 5840R, Germany). The serum was separated and frozen at − 20 °C. Two birds in each cage of each group were randomly selected and sacrificed. Among them, the thyroid samples of two birds from two different cages in each group were extracted, immediately placed into 10% buffered formalin (pH 7.4) and stored at 4 °C for further treatment, the other thyroid tissues from ten birds in different groups were frozen into liquid nitrogen and stored at − 80 °C for further analysis.

2.3. Tissue pathological observation

Thyroid tissue soaked in 10% buffered formalin was treated with conventional methods of embedding, slicing, and hematoxylin-eosin staining. Briefly, a tissue block was transferred to alcohol for dehydration and to xylene for solvent replacement. Subsequently, the tissue block was embedded in melted paraffin, fixed on the slicer, and cut to 5 μm flakes in thickness. After that, the sections were soaked in a mixture of xylene and alcohol for dewaxing and stained by hematoxylin and 0.5% eosin alcohol. Finally, the sections were dehydrated with alcohol and xylene, and sealed by adding gum. Stained sections were observed under a bright field optical microscope and photographed (Olympus Optical Co., Japan).

2.4. Total RNA extraction and cDNA library preparation

Thyroid samples stored at − 80 °C from the 4 g/kg and control groups were collected, and total RNA was extracted from eight broilers according to the mirVana miRNA Isolation Kit manufacturer's specifications (cat.no:1561, Ambion, USA). Then, mRNA integrity was evaluated by using an Agilent 2100 Bioanalyzer (Agilent Technologies, CA, USA), and subsequent analysis was performed based on the samples with RNA integrity number ≥ 7. After purifying mRNA, the synthesis of cDNA was conducted using SuperScript II Reverse Transcriptase (cat. no:18064014, Invitrogen, USA). For high-throughput RNA-Seq, strand-specific cDNA libraries were constructed following to the TruSeq Stranded mRNA LTSample Prep Kit manufacturer's instructions (cat.no: RS-122–2101, Illumina, USA), and sequencing was performed on an Illumina HiSeqTM 2500 platform by OE Biotech Co., Ltd (Shanghai, China).

2.5. Quality control and mapping

The original raw data were saved in FASTQ/FQ fle format. Quality control and trimming were performed after proper quality control of the raw data using Trimmomatic to remove any poly-N and low-quality reads. Then, the clean reads were mapped to the reference genome using hisat2 (Kim et al., 2015). The transcript-level was quantified by fragments per kilobase per million (FPKM) method using bowtie2c, and the read counts of each transcript (protein_coding) were obtained using eXpress (Trapnell et al., 2010).

2.6. Differential gene expression and functional enrichment analysis

Basing on the FPKM value and read counts of each transcript, the differentially expressed genes (DEGs) between 4 g/kg and control groups (n = 3 per group) were screened out using DESeq functions estimateSizeFactors and nbinomTest. Then, the heat map analysis and volcano plot of DEGs were performed with R and DESeq software. A transcript was considered to be differentially expressed if $P < 0.05$ and $|\log_2 \text{fold change}| > 0.58$. Subsequently, to describe the functional classification of genes and discover the link between DEGs, hierarchical cluster analysis of DEGs was performed using R based on the Gene Ontology (GO) and Kyoto Encyclopaedia of Genes and Genomes (KEGG) databases (http://www.genome.jp/kegg) (Kanehisa et al., 2008).

2.7. QRT-PCR

Using the total RNA obtained from thyroid tissue samples, the yield of RNA was determined using a NanoDrop 2000 spectrophotometer (Thermo Scientific, USA), and integrity was evaluated using agarose gel

electrophoresis stained with ethidium bromide. Then, TransScript All-in-One First-Strand cDNA Synthesis SuperMIX for reverse transcription PCR (TransGen Biotech, China) was used to remove the genomic DNA and synthesize cDNA. Each RT reaction had two steps: first, 0.5 μg RNA and 2 μL of 4 × gDNA wiper Mix were added to 8 μL of nuclease-free H_2O, with reactions performed in a GeneAmp® PCR System 9700 (Applied Biosystems, USA) for 2 min at 42 °C; and second, 2 μL of 5 ×HiScript II QRT SuperMix IIa was added into the reaction system and treated in a GeneAmp® PCR System 9700 for 15 min at 50 °C and 5 s at 85 °C. A total of 10 μL of RT reaction mixture was then diluted 10 times with nuclease-free water and held at − 20 °C.

The QRT-PCR was performed with 10 μL of PCR reaction system, including reaction mixture that included 1 μL of cDNA, 5 μL of PerfectStart™ Green qPCR SuperMix (TransGen Biotech, China), 0.2 μL of forward primer, 0.2 μL of reverse primer, and 3.6 μL of nuclease-free water using Light Cycler® 480 II Real-time PCR Instrument (Roche, Swiss). The QRT-PCR conditions included: pre-denaturation at 95 °C for 30 s, followed by 40 cycles of denaturation at 95 °C for 10 s, annealing at 60 °C for 30 s, and elongation at 72 °C for 20 s. All samples were run in triplicate. Melting curve analysis was performed to validate the specific generation of the expected PCR product. Relative gene expression levels were quantified using the $2^{-\Delta\Delta Ct}$ method compared with *β-actin*. Primer sequences for QRT-PCR were designed in the laboratory and synthesized by OE Biotech Co., Ltd based on the mRNA sequences obtained from the NCBI database, and were given in Table S3.

2.8. ELISA measurements

In each group, the blood samples were collected into tubes containing anticoagulant (heparin) and centrifuged at 700 g for 10 min at 4 °C to separate serum. The levels of T3 (cat.no: MM-34263O1), T4 (cat.no: MM-34207O1), free triiodothyronine (FT3, cat.no: MM-33324O1), free thyroxine (FT4, cat.no: MM-33323O1), thyroid stimulating hormone (TSH, cat.no: MM-2297O1), and 5′-deiodinase (ID, cat.no: MM-34279Q1) in serum were examined using commercially available ELISA kits according to the manufacturer's recommendations (MEIMIAN, China). All samples were run in triplicate.

2.9. Data analysis

All data were presented as means ± standard deviation (SD) and analyzed using SPSS (version 16.0) software. One-way ANOVA was used to determine significant differences among different groups. Differences were considered significant at $P < 0.05$. Spearman's rank correlation coefficient analysis was used to further show the correlations between exposure concentrations of BDE-209 and the levels of thyroid hormones.

3. Results

3.1. Thyroid microstructure

When Arbor Acres broiler chicks were fed with basal diet containing different concentrations of BDE-209, histopathologic changes were observed in thyroid tissue combining with Image Pro Plus software analysis (version 6.0, Table S4). In the control group, the structure of thyroid follicls was clear (Fig. 1A). After exposure to different concentrations of BDE-209, the number of thyroid follicls were increased (Fig. 1B-E) by comparing with control group, and the volume was reduced obviously (Fig. 1D–E). Further more, in Fig. 1C-E, follicular epithelial cells became swollen, eventually ruptured and pyknotic; and many crumpled outer walls of irregular follicles formed new follicles and crumple. This result indicated that the histological structure of thyroid tissue was damaged by supplemental feeding of BDE-209, and was even hyperplastic (Salabè, 2001; Miura and Mineta, 2014).

3.2. Transcriptome sequencing and assembly

Based on the damages to thyroid histological structure, the transcriptome characteristics of thyroid tissue were determined using RNA-Seq analysis. After removing adapter sequences, undetermined bases, and low-quality reads, more than 48,880,000 clean reads were obtained in each sampling group. The Q30 and GC were more than 95.49% and 46.14%, respectively (Table S5). Then, the clean reads were mapped into the specified reference genome using Hisat2 to obtain position information on the reference genome or gene, and the sequence characteristic information was unique to the sequencing sample. Statistical analysis of reference genome alignment reads showed that the percentage of total mapped exceeded 70%, and multiple mapped sequences represented less than 10%. The above results indicated that the sequence data were of high quality and could be used for subsequent data analysis.

3.3. Analysis of DEGs

After calculating the FPKM value of each gene using bowtie2c and obtaining the read counts of each gene by eXpress, significant DEGs were identified using the DESeq R package functions estimate based on the thresholds of $P < 0.05$ and $|\log_2 \text{fold change}| > 0.58$. The hierarchical clustering for the DEGs between thyroid samples of 4 g/kg BDE-209 group (T4) and thyroid samples of control group (Tck) showed express genes differently relative to the control (Fig. 2A), red represented up-regulation and blue represented down-regulation. And a total of 501 DEGs were identified between the 4 g/kg BDE-209 and control groups: 222 upregulated and 279 downregulated, and all these DEGs were represented on a volcano plot map ($\log_{10} P$ value vs $-\log_2$ fold change). The foldchanges and P value of these DEGs were list in Fig. 2A, red and green dots indicate upregulation and downregulation of DEGs in the BDE-209-exposed group, respectively. The larger the $|\log_2$ fold change$|$ and $-\log_{10} P$ value, the more significant genes.

3.4. GO and KEGG enrichment analysis

To explore the critical functions affected by BDE-209, all DEGs were mapped to three categories of gene ontology (GO), which included biological processes (1629 subclasses), cellular components (298), and molecular functions (528). The top 30 terms and were list in Fig. 3 (Table S6), the larger enrichment score and the $-\log_{10} P$ value represented the more significant term, such as cellular response to stress (3 genes, *P* value 1.45E-06, enrichment score 21.56), regulation of cilium beat frequency (3 genes, *P* value 1.45E-06, enrichment score 21.56), parathyroid gland development (3 genes, *P* value 1.45E-06, enrichment score 21.56), and cellular response to vitamin D (3 genes, *P* value 1.45E-06, enrichment score 21.56) in biological processes; extracellular space (48 genes, *P* value 5.89E-05, enrichment score 1.75), plasma membrane (120 genes, *P* value 9.84E-05, enrichment score 1.36), extracellular region (48 genes, *P* value 1.34E-04, enrichment score 1.69), and microvillus (6 genes, *P* value 1.40E-04, enrichment score 5.07) in cellular component; and structural molecule activity (14 genes, *P* value 4.17E-05, enrichment score 3.12), potassium channel activity (5 genes, *P* value 2.18E-04, enrichment score 5.53), guanylate cyclase activity (4 genes, *P* value 2.93E-04, enrichment score 6.39), and G-protein coupled peptide receptor activity (3 genes, *P* value 3.93E-04, enrichment score 7.84) in molecular function.

In addition, based on the Database for Annotation, Visualization and Integrated Discovery (DAVID), DEGs were found to be significantly enriched in many KEGG pathways, including neuroactive ligand-receptor interaction (8 genes, *P* value 5.36E-08, enrichment score 2.90), cell adhesion molecules CAMs (12 genes, *P* value 5.65E-05, enrichment score 3.30), vascular smooth muscle contraction (11 genes, *P* value 3.33E-04, enrichment score 2.92), the calcium signaling pathway (11 genes, *P* value 9.76E-03, enrichment score 1.96), and steroid biosynthesis (4 genes, *P* value 1.59E-04, enrichment score 7.18) and

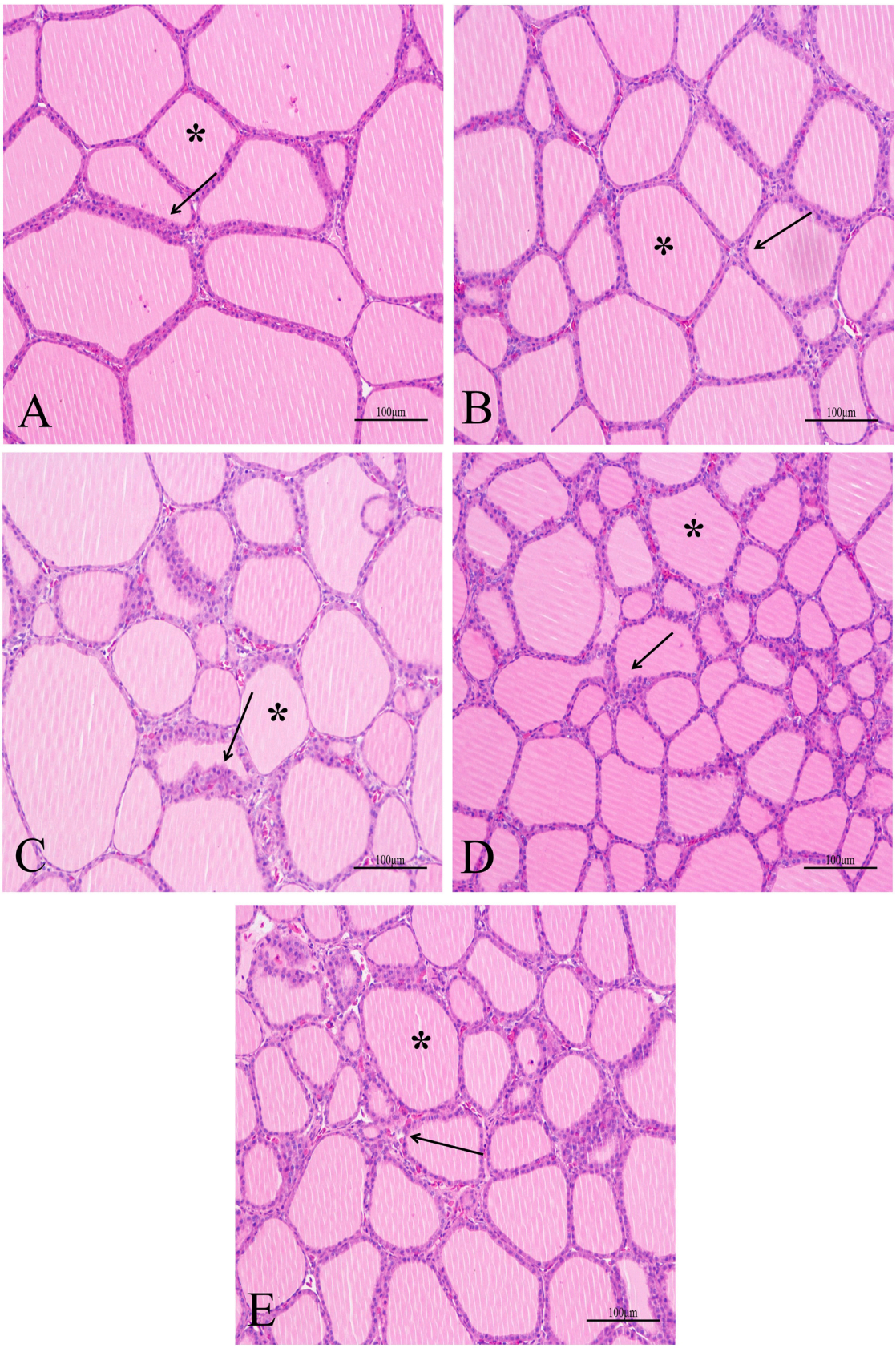

Fig. 1. Histological changes of thyroid tissues from broiler chicks after treatment with different concentrations of BDE-209 for 6 weeks. Note: (A) control group; (B) 0.004 g/kg BDE-209 group; (C) 0.04 g/kg BDE-209 group; (D) 0.4 g/kg BDE-209 group; and (E) 4 g/kg BDE-209 group. Asterisk represented the thyroid follicles, and the arrow represented the follicular epithelial cells.

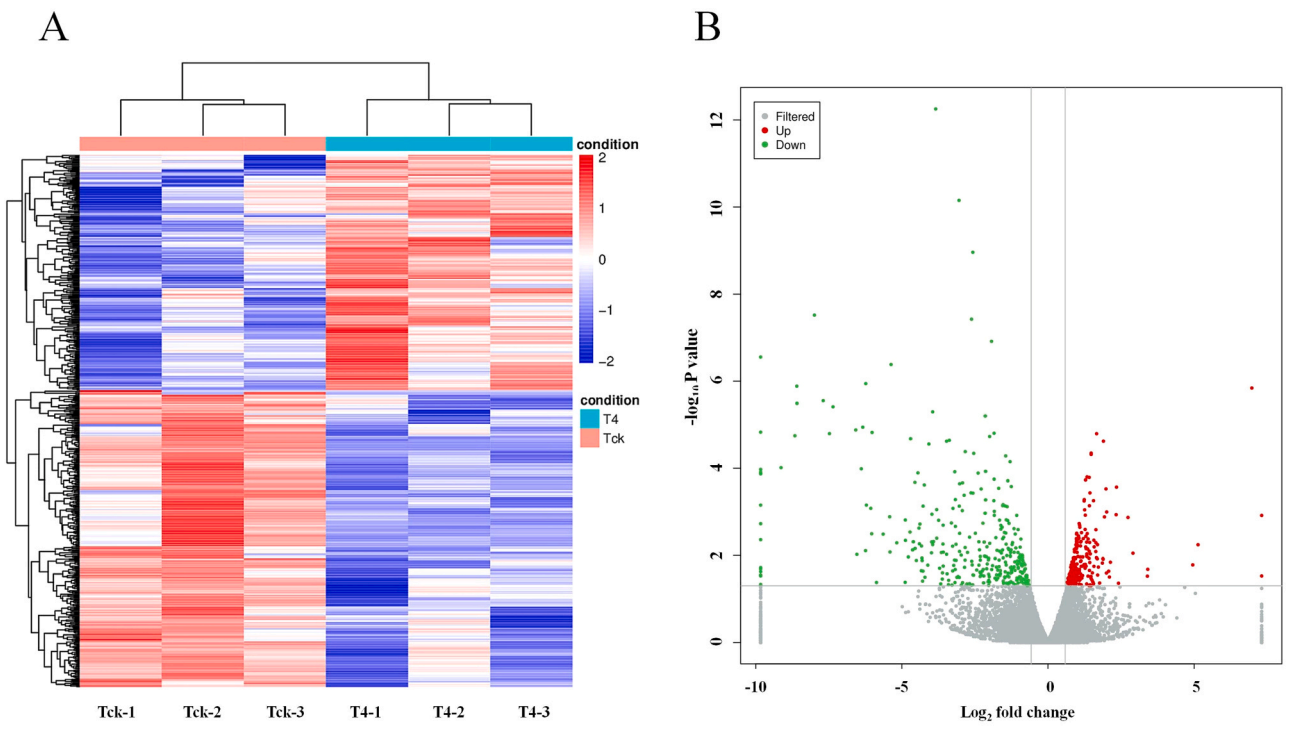

Fig. 2. Heat map analysis (A) and volcano plot (B) of DEGs between the control group (Tck, n = 3) and the 4 g/kg BDE-209 treatment group (T4, n = 3). In figure A, higher expression genes are shown in red and low expression genes are shown in blue. In figure B, X-axis is the $\log_2$ fold change, and Y-axis is the $-\log_{10} P$ value; gray displays non-significant differences, red displays upregulated genes and green displays downregulated genes.

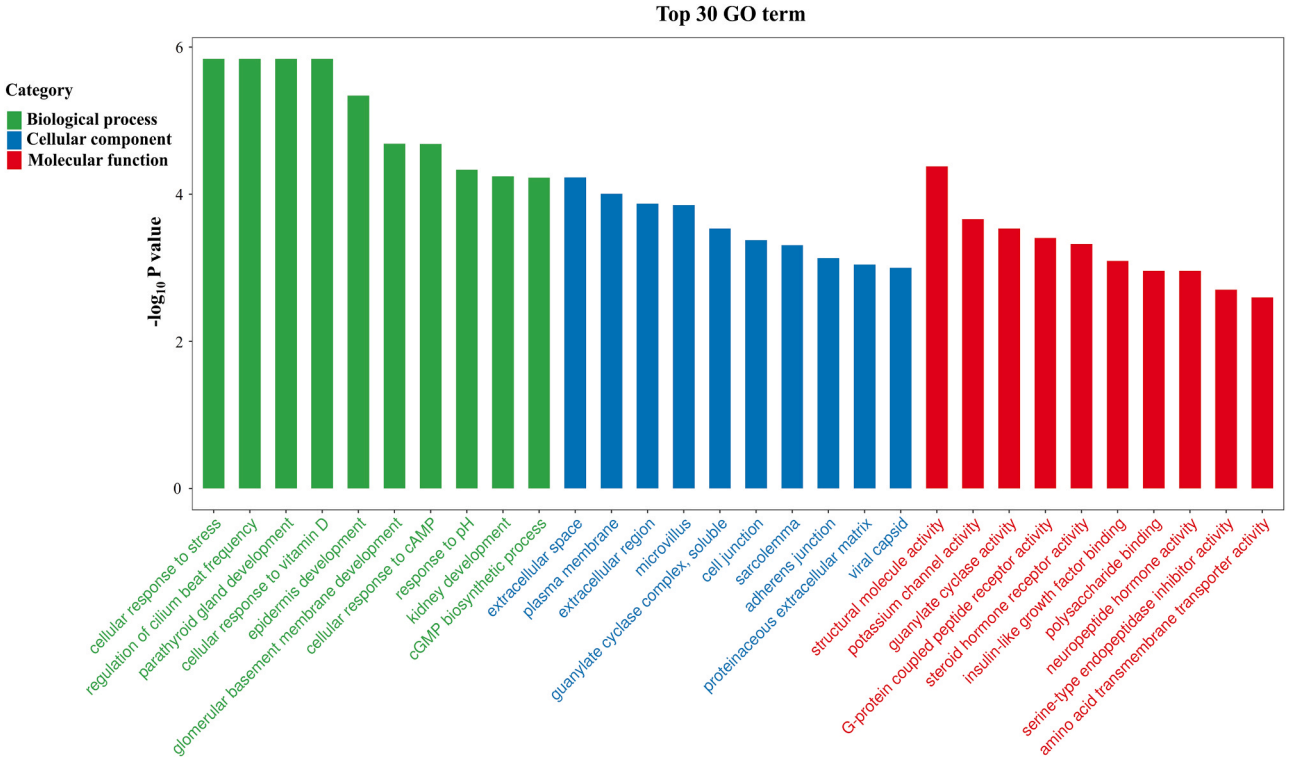

Fig. 3. Gene ontological classifications of differentially expressed genes (DEGs) between the 4 g/kg BDE-209 treatment and control groups. X- axis is the name of Go terms and the Y- axis is $-\log_{10}$ P value.The DEGs are grouped into three hierarchically stretched GO terms: biological process (green), cellular components (blue), and molecular functions (red).

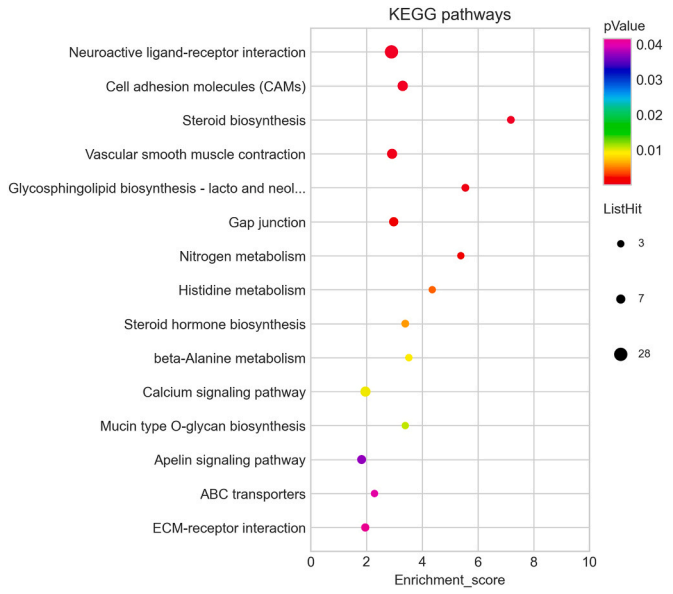

Fig. 4. KEGG pathway enrichment scatter plot. The size of the *P* value is represented by color of the point, and the number of DEGs included in each pathway is expressed by the size of the point.

so on (Fig. 4 and Table S7).

Among these KEGG pathways, seven relevant hormone receptors enriched in the neuroactive ligand-receptor interaction pathway were selected for further QRT-PCR analysis, including five upregulated genes with quantitative expression value >1: α1D-adrenergic receptor (*ADRA1D*, relative quantitative expression value 3.78), follicle-stimulating hormone receptor (*FSHR*, 7.23), prolactin receptor (*PRLR*, 3.20), prostaglandin F receptor (*PTGFR*, 1.80) and thyroid stimulating hormone receptor (*TSHR*, 2.84); and two downregulated genes with quantitative expression value <1: somatostatin receptor type 2 (*SSTR2*, 0.85) and glucagon-like peptide 2 receptor (*GLP2R*, 0.28). The trends of the QRT-PCR and RNA-Seq results were consistent, indicating that the sequencing results were accurate and reliable (Fig. 5 and Table S8).

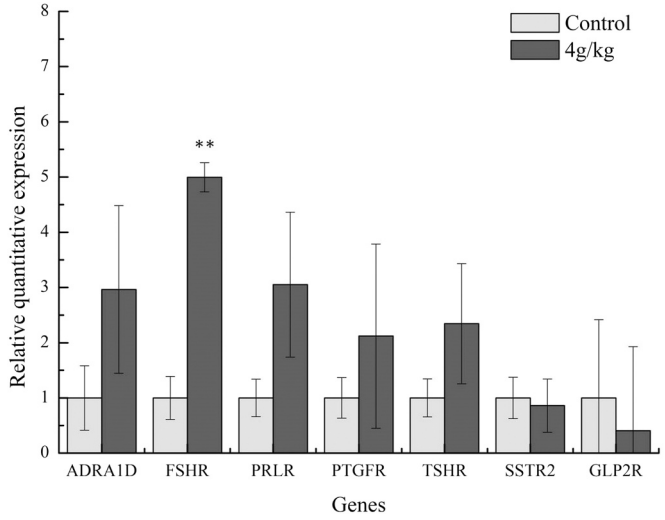

Fig. 5. Validation of seven selected DEGs by using real-time PCR. Note: the relative quantitative expression value (mean ± SD, n = 3) of these genes in 4 g/kg group were normalized to these expression values in control group, and the relative quantitative expression values in control group were all equal to 1. ** represents significant difference with *P* value <0.01 compared to control group.

3.5. Thyroid hormone levels in serum after BDE-209 treatment

Moreover, according to the differential expression of seven hormone receptors in thyroid after BDE-209 exposure, the levels of FT3, FT4, T3, T4, ID, and TSH in the serum of broilers were shown in Fig. 6. Compared to control group, significant decreases in FT3, T4, and TSH levels were observed in all BDE-209 treatment groups ($P < 0.05$; Fig. 6A, D, and F); FT4 and ID levels were significantly reduced in higher BDE-209 concentration groups (0.4 and/or 4 g/kg, Fig. 6B and E). However, no significant difference was observed in T3 for all BDE-209 treatment groups compared with control ($P > 0.05$; Fig. 6C). Furthermore, there was a significant Spearman's correlation coefficient (−1) between T4 levels and concentrations of BDE-209 treatment.

4. Discussion

As reported in previous studies, PBDEs are one type of disruptor of the hypothalamic-pituitary-thyroid (HPT) axis. Due to their similar structure to thyroid hormones, it has been hypothesized that PBDEs may interfere with the transport and metabolism of thyroid hormones (McDonald, 2002; Birnbaum and Staskal, 2004). In adult fathead minnows (*Pimephales promelas*), dietary exposure to BDE-47 altered T4 signaling at multiple levels of the HPT axis, which suggested that thyroid hormone-responsive pathways in the brain may be particularly sensitive to disruption by PBDEs (Lema et al., 2008). These findings indicated that neurogenesis and brain development may be impacted by PBDEs exposure, and how PBDEs influence thyroid hormone-mediated neural function remains unclear.

In the present study, the microstructure of thyroid tissue was significantly changed in broiler chicks after supplemental feeding with BDE-209, including increased number and reduced volume of thyroid follicls, irregular and deformed follicular cells, followed by ruptured and pyknotic follicular epithelial cells (Fig. 1). This result was in agreement with previous studies, which also reported negative effects of BDE-209 or PBDEs on the thyroid of organisms (Wang et al., 2019). Furthermore, the transcriptomic analysis of the thyroid exposed to 4 g/kg BDE-209 revealed 501 DEGs (222 upregulated and 279 downregulated). The KEGG pathway enrichment analysis showed that neuroactive ligand-receptor interaction (http://www.genome.jp/kegg/pathway/hsa/hsa04080.html) was the most significant pathway (8 genes, *P* value 5.36E-08, see Fig. 4). In antipsychotic treatment response, neuroactive ligand-receptor interaction pathways were also found to be enriched using SNP-based analysis (Adkins et al., 2012). For Parkinson's disease, α-synuclein could induce the dysregulation of miRNAs, and the neuroactive ligand-receptor interaction pathway was most likely affected by these miRNAs (Kong et al., 2015). Additionally, SiO_2 nanoparticles can induce developmental neurotoxicity by affecting the neuroactive ligand-receptor interaction signaling pathway (Wei et al., 2020). These different types of evidences suggest that the neuroactive ligand-receptor interaction pathway plays an important role in stress responses.

From the neuroactive ligand-receptor interaction list, we identified all known genes encoding receptors for each ligand and screened out seven key DEGs: *ADRA1D*, *FSHR*, *PRLR*, *PTGFR*, *TSHR*, *SSTR2* and *GLP2R*. The QRT-PCR results were consistent with the transcriptomic data, and showed upregulated expression levels of *ADRA1D* (relative quantitative expression value 3.78), *FSHR* (7.23), *PRLR* (3.20), *PTGFR* (1.80) *and TSHR* (2.84), and downregulated levels of *SSTR2* (0.85) and *GLP2R* (0.28) after BDE-209 treatment (Fig. 5, Table S8). Among them, α1-adrenergic receptors (α1-ARs) belong to class I of the G-protein coupled receptor superfamily. They mainly mediate responses to epinephrine and norepinephrine, abnormalities in regulation of α1-ARs have been reported to contribute to the development of hypertension and heart failure (García-Cazarín et al., 2008). In a previous study, TSH showed the ability to increase the number of α1-ARs by inducing their biosynthesis, and this was linked to the formation of thyroid hormones (Corda and Kohn, 1985). Thyroid hormones were shown to play a role in

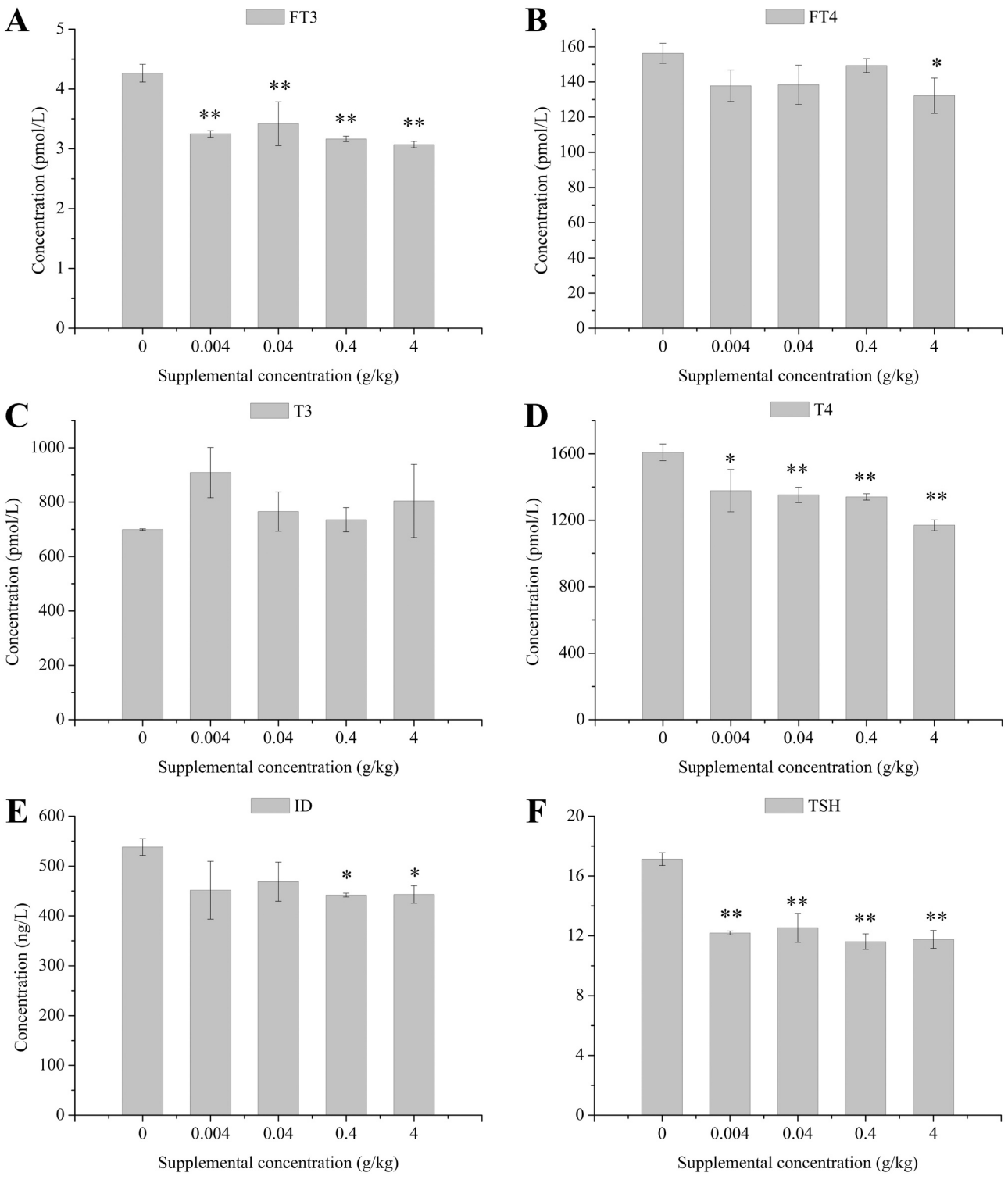

Fig. 6. A: FT3, free triiodothyronine; B: FT4, free thyroxine; C: T3, triiodothyronine; D: T4, thyroxine; E: ID, deiodinase; F: TSH, thyroid stimulating hormone.

the control of cardiac adrenergic receptor expression during a critical development period (Metz et al., 1996), but limited research has investigated the interaction between *ADRA1D* and TSH. Combined with the decreased the levels of T4 and TSH in this study after BDE-209 exposure (Fig. 6D and E), we deduced that the up-regulated *ADRA1D* may participate in compensatory effects related to the inhibited formation of TSH and T4 induced by BDE-209. However, the detailed regulatory mechanism needs further study.

In addition, both *FSHR* and *TSHR* also belong to the G-protein coupled receptor superfamily, playing a physiological role through mediating the cAMP pathway (Segaloff and Ascoli, 2013). Previous study demonstrated positive FSHR immunostaining in some follicles of hyperplasia nodularis or thyroid adenomas, and ectopic *FSHR* may constitute a novel biomarker and target in the treatment of cancer, including thyroid cancer (Pawlikowski et al., 2015). Besides, *FSHR* immunopositivity was observed in 87.5% of follicular cancers, papillary cancers and all the examined undifferentiated cancers, and serum FSH level was increased in thyroid adenoma as well as *FSHR* expression (Liu

et al., 2014). The present study also showed upregulated expression of *FSHR* in thyroid of broiler chicks by supplemental feeding with BDE-209 (Fig. 5), suggesting thyroid adenoma resulted from exposure to 4 g/kg BDE-209.

For *TSHR*, locating at the basolateral membrane of thyroid follicular cells, is critical in the development, growth and function of the thyroid, and is involved in the signal transfer mediated by Gαs and Gαq (Szkudlinski et al., 2002). It has been demonstrated that TSH can positively modulate TSHR in normal cells up to a certain limit, and downregulates TSHR at high concentrations (Akamizu et al., 1990). Binding of TSH to TSHR stimulates thyroid-epithelial cell proliferation and regulates the expression of differentiation marker thyroglobulin (Tg), which is necessary for the synthesis of thyroid hormones, and TSHR-mRNA and Tg-mRNA in peripheral blood have been reported to be equally sensitive and specific markers for thyroid cancer (Gupta et al., 2020). Moreover, a lack of expression of TSHR has been considered as a significant independent factor affecting distant metastasis and poor prognosis in differentiated thyroid cancer (Liu et al., 2017). In this study, *TSHR* transcriptional level in thyroid was increased after BDE-209 exposure, while significantly decreased levels of thyroid hormones (FT4, FT3, T4 and TSH) were observed in serum (Fig. 6). In fact, the HPT axis is involved in the regulation of cell differentiation, growth, and metabolism in different areas of the central nervous system and in the peripheral tissues of vertebrates (Zoeller et al., 2007), and is regulated by several complex feedback mechanisms at all levels, among them, free T3 and T4 feedback at the anterior pituitary level to inhibit TSH release (Chakrabarti, 2011). Hence, we inferred that BDE-209 exposure can impact the feedback modulation between free T3 and T4at the anterior pituitary level to impact TSH levels, and then influence the feedback regulation on TSHR expression.

Somatostatin receptors (*SSTRs*) have five subtypes (*SSTR1–SSTR5*) with multiple functions, including inhibitory effects on cell survival and angiogenesis and antiproliferative effects on cancer cell lines (Herac et al., 2016). Among them, SSTR2 has been shown to be predominantly expressed in some neuroendocrine tumors, and is characteristic for somatotroph pituitary adenomas (Mato et al., 1998; Chinezu et al., 2014). Generally, SSTR scintigraphy is a reliable, non-invasive and highly sensitive procedure for detection of metastatic differentiated thyroid carcinoma (Haslinghuis et al., 2001), and for benign and malignant thyroid tissue but not in normal tissue (Atkinson et al., 2013). However, in hypothyroid rats, the mRNA level of SSTR2 was significantly reduced in the pituitary, and the reduction could be prevented by T4 supplementation, revealing feedback regulation between thyroid hormones SSTR subtypes expression in the pituitary (Lam and Wong, 1999). Besides, negative feedback exerted by the increasing plasma T3 levels toward chicken hatching has been supposed to be partly mediated by increased expression of SSTR2 and SSTR5 (Groef et al., 2007). In this study, the result indicated downregulated expression of SSTR2 in the thyroid after supplemental feeding with 4 g/kg BDE-209 (Fig. 5), and the level of T4 in serum was clearly inhibited (Fig. 6D), but no significant change in T3 level (Fig. 6D). Therefore, we speculated that supplemental feeding of BDE-209 to broilers causes an adverse effect on feedback regulation between SSTR2 and thyroid hormones, and results in hypothyroid and even thyroid tumor, but the underlying mechanism of PBDE exposure needs to be elucidated.

In addition, the levels of FT3, T4, and TSH in serum were significantly decreased following BDE-209 treatment, as well as FT4 and ID levels under higher BDE-209 concentrations, and a significant correlation was observed between T4 levels and exposure concentrations (Fig. 6). This indicated the inhibition effects of BDE-209 on thyroid hormones of chicks. In previous studies, Tebourbi et al. (2010) found that the T4 level and 5′-ID activity of male Wistar rats were decreased after intraperitoneal injection with p,p′-DDT; T3 and T4 levels were both reduced after BDE-209 exposure in zebrafish larvae (Chen et al., 2012) and fathead minnows (Noyes et al., 2013). Recently, the associations of low exposure of persistent organic pollutants (POPs) with thyroid hormones were measured in human breast milk, including PBDEs, polychlorinated biphenyls and dioxins, and a significantly decreased trend in thyroid hormones with increasing exposure to POPs was demonstrated (Li et al., 2019). Combinding with the significant epression of above DEGs in neuroactive ligand-receptor interaction pathway, we deduced the disturbtion of feedback regulation between critical receptors genes in the neuroactive ligand-receptor interaction pathway and thyroid hormones, leading to toxic effects of thyroid of chicks.

5. Conclusion

The present study provided evidence that supplemental feeding with BDE-209 caused the obviously pathological changes of thyroid tissue in broiler chicks, including deformed and increased follicular cells, swollen and even ruptured follicular epithelial cells, as well as new follicles and crumple from irregular follicles. The neuroactive ligand-receptor interaction pathway was the most significantly enriched signal pathway in the thyroid after 4 g/kg BDE-209 exposure according to transcriptomic analysis. Combined with the significantly decreased levels of FT3, T4, ID, and TSH in serum, the expression levels of *ADRA1D*, *FSHR*, *TSHR*, and *SSTR2* genes in thyroid and T4 level in serum could be potential candidate biomarkers. Overall, these results provide evidence that oral intake of the brominated flame-retardant BDE-209 can cause structural injuries and even hyperplasia, and illustrate how BDE-209 induces changes in thyroid hormones and their regulated gene transcription in the broiler thyroid by the neuroactive ligand-receptor interaction pathway. These insights into toxic biomarkers can provide a theoretical basis for rapid diagnosis of PBDEs in broiler chicks, other animals, and even humans. However, future investigations into how PBDEs influence the thyroid hormone-mediated neural function pathway are needed.

CRediT authorship contribution statement

Lin Cheng: Conceptualization, Data curation, Formal analysis, Writing - original draft. **Junhua Yang:** Investigation, Methodology, Data curation. **Qinxiong Rao:** Investigation, Supervision. **Zehui Liu:** Methodology, Visualization. **Wei Song:** Formal analysis. **Shuhui Guan:** Data curation. **Zhihui Zhao:** Conceptualization, Investigation, Project administration, Supervision. **Weiguo Song:** Conceptualization, Methodology, Project administration, Writing - review & editing.

Declaration of Competing Interest

The authors declare that they have no known competing financial interests or personal relationships that could have appeared to influence the work reported in this paper.

Acknowledgements

The authors acknowledge the financial support by National Key Research and Development Program of China (2017YFC1600302) and the platform provided by Shanghai Engineering Research Center for Agro-food Quality and Safety.

Appendix A. Supporting information

Supplementary data associated with this article can be found in the online version at doi:10.1016/j.ecoenv.2021.112305.

References

Adkins, D.E., Khachane, A.N., Mcclay, J.L., Aberg, K., Bukszár, J., Sullivan, P.F., van den Oord, E.J., 2012. SNP-based analysis of neuroactive ligand–receptor interaction pathways implicates PGE2 as a novel mediator of antipsychotic treatment response: data from the CATIE study. Schizophr. Res. 135 (1–3), 200–201.

Akamizu, T., Ikuyama, S., Saji, M., Kosugi, S., Kozak, C., McBride, O.W., Kohn, L.D., 1990. Cloning, chromosomal assignment, and regulation of the rat thyrotropin

receptor: expression of the gene is regulated by thyrotropin, agents that increase camp levels, and thyroid autoantibodies. Proc. Natl. Acad. Sci. USA 87 (15), 5677–5681.
Atkinson, H., England, J.A., Rafferty, A., Jesudason, V., Bedford, K., Karsai, L., Atkin, S. L., 2013. Somatostatin receptor expression in thyroid disease. Int. J. Exp. Pathol. 94, 226–229.
Birnbaum, L.S., Staskal, D.F., 2004. Brominated flame retardants: cause for concern? Environ. Health Perspect. 112 (1), 9–17.
Chakrabarti, S., 2011. Thyroid functions and bipolar affective disorder. J. Thyroid Res. 2011, 1–13.
Chen, D., La Guardia, M.J., Harvey, E., Amaral, M., Wohlfort, K., Hale, R.C., 2008. Polybrominated diphenyl ethers in peregrine falcon (Falco peregrinus) eggs from the northeastern U.S. Environ. Sci. Technol. 42 (20), 7594–7600.
Chen, T., Niu, P., Kong, F., Wang, Y., Bai, Y., Yu, D., Jia, J., Yang, L., Fu, Z., Li, R., Li, J., Tian, L., Sun, Z., Wang, D., Shi, Z., 2018. Disruption of thyroid hormone levels by decabrominated diphenyl ethers (BDE-209) in occupational workers from a deca-BDE manufacturing plant. Environ. Int. 120, 505–515.
Chen, Q., Yu, L., Yang, L., Zhou, B., 2012. Bioconcentration and metabolism of decabromodiphenyl ether (BDE-209) result in thyroid endocrine disruption in zebrafish larvae. Aquat. Toxicol. 110–111, 141–148.
Chinezu, L., Vasiljevic, A., Jouanneau, E., François, P., Borda, A., Trouillas, J., Raverot, G., 2014. Expression of somatostatin receptors, SSTR2A and SSTR5, in 108 endocrine pituitary tumors using immunohistochemical detection with new specific monoclonal antibodies. Hum. Pathol. 45 (1), 71–77.
Corda, D., Kohn, L.D., 1985. Thyrotropin upregulates alpha 1-adrenergic receptors in rat FRTL-5 thyroid cells. Proc. Natl. Acad. Sci. USA 82 (24), 8677–8680.
Covaci, A., Harrad, S., Abdallah, M.A., Ali, N., Law, R.J., Herzke, D., de Wit, C.A., 2011. Novel brominated flame retardants: a review of their analysis, environmental fate and behaviour. Environ. Int. 37 (2), 532–556.
Darnerud, P.O., 2008. Brominated flame retardants as possible endocrine disrupters. Int. J. Androl. 31 (2), 152–160.
García-Cazarín, M.L., Smith, J.L., Olszewski, K.A., McCune, D.F., Simmerman, L.A., Hadley, R.W., Kraner, S.D., Piascik, M.T., 2008. The alpha1D-adrenergic receptor is expressed intracellularly and coupled to increases in intracellular calcium and reactive oxygen species in human aortic smooth muscle cells. J. Mol. Signal. 3 (3), 6.
Groef, B.D., Grommen, S.V.H., Darras, V.M., 2007. Feedback control of thyrotropin secretion in the chicken: thyroid hormones increase the expression of hypophyseal somatostatin receptor types 2 and 5. Gen. Comp. Endocrinol. 152 (2–3), 178–182.
Gupta, M.K., Taguba, L., Arciaga, R., Siperstein, A., Faiman, C., Mehta, A., Reddy, S.S.K., 2020. Detection of circulating thyroid cancer cells by reverse transcription-PCR for thyroid-stimulating hormone receptor and thyroglobulin: the importance of primer selection. Clin. Chem. 48 (10), 1862–1865.
Haslinghuis, L.M., Krenning, E.P., De Herder, W.W., Reijs, A.E., Kwekkeboom, D.J., 2001. Somatostatin receptor scintigraphy in the follow-up of patients with differentiated thyroid cancer. J. Endocrinol. Investig. 24 (6), 415–422.
Herac, M., Niederle, B., Raderer, M., Krebs, M., Kaserer, K., Koperek, O., 2016. Expression of somatostatin receptor 2A in medullary thyroid carcinoma is associated with lymph node metastasis. APMIS: Acta Pathol., Microbiol., Et. Immunol. Scand. 124 (10), 839–845.
Kanehisa, M., Araki, M., Goto, S., Hattori, M., Hirakawa, M., Itoh, M., Katayama, T., Kawashima, S., Okuda, S., Tokimatsu, T., Yamanishi, Y., 2008. KEGG for linking genomes to life and the environment. Nucleic Acids Res. 36, 480–484.
Kim, D., Langmead, B., Salzberg, S.L., 2015. HISAT: a fast spliced aligner with low memory requirements. Nat. Methods 12 (4), 357–360.
Kim, T.H., Lee, Y.J., Lee, E., Kim, M.S., Kwack, S.J., Kim, K.B., Chung, K.K., Kang, T.S., Han, S.Y., Lee, J., Lee, B.M., Kim, H.S., 2009. Effects of gestational exposure to decabromodiphenyl ether on reproductive parameters, thyroid hormone levels, and neuronal development in sprague-dawley rats offspring. J. Toxicol. Environ. Health Part A 72 (21–22), 1296–1303.
Kong, Y., Liang, X., Liu, L., Zhang, D., Wan, C., Gan, Z., Yuan, L., 2015. High throughput sequencing identifies micrornas mediating α-synuclein toxicity by targeting neuroactive-ligand receptor interaction pathway in early stage of drosophila parkinson's disease model. Plos One 10 (9), 0137432.
Labunska, I., Harrad, S., Santillo, D., Johnston, P., Yun, L., 2013. Domestic duck eggs: an important pathway of human exposure to PBDEs around e-waste and scrap metal processing areas in Eastern China. Environ. Sci. Technol. 47 (16), 9258–9266.
Lam, K.S., Wong, R.L., 1999. Thyroid hormones regulate the expression of somatostatin receptor subtypes in the rat pituitary. Neuroendocrinology 69 (6), 460–464.
Lema, S.C., Dickey, J.T., Schultz, I.R., Swanson, P., 2008. Dietary exposure to 2,2′,4,4′-Tetrabromodiphenyl Ether (PBDE-47) alters thyroid status and thyroid hormone-regulated gene transcription in the pituitary and brain. Environ. Health Perspect. 116 (12), 1694–1699.
Liu, J., Chen, G., Meng, X.Y., Liu, Z.H., Dong, S., 2014. Serum levels of sex hormones and expression of their receptors in thyroid tissue in female patients with various types of thyroid neoplasms. Pathol. Res. Pract. 210 (10), 830–835.
Liu, T., Men, Q., Su, X., Chen, W., Zou, L., Li, Q., Song, M., Ouyang, D., Chen, Y., Li, Z., Fu, X., Yang, A., 2017. Downregulated expression of TSHR is associated with distant metastasis in thyroid cancer. Oncol. Lett. 14 (6), 7506–7512.
Li, Z.M., Albrecht, M., Fromme, H., Schramm, K.W., De Angelis, M., 2019. Persistent organic pollutants in human breast milk and associations with maternal thyroid hormone homeostasis. Environ. Sci. Technol. 54 (2), 1111–1119.
Li, X., Dong, S., Zhang, W., Fan, X., Li, Y., Wang, R., Su, X., 2018. Global occurrence of polybrominated diphenyl ethers and their hydroxylated and methoxylated structural analogues in an important animal feed (fishmeal). Environ. Pollut. 234, 620–629.
Luo, X.J., Liu, J., Luo, Y., Zhang, X.L., Wu, J.P., Lin, Z., Chen, S.J., Mai, B.X., Yang, Z.Y., 2009. Polybrominated diphenyl ethers (PBDEs) in free-range domestic fowl from an e-waste recycling site in South China: Levels, profile and human dietary exposure. Environ. Int. 35 (2), 253–258.
Mato, E., Matías-Guiu, X., Chico, A., Webb, S.M., Cabezas, R., Berná, L., De Leiva, A., 1998. Somatostatin and somatostatin receptor subtype gene expression in medullary thyroid carcinoma1. J. Clin. Endocrinol. Metab. 83 (7), 2417–2420.
McDonald, T.A., 2002. A perspective on the potential health risks of PBDEs. Chemosphere 46, 745–755.
Metz, L.D., Seidler, F.J., Mccook, E.C., Slotkin, T.A., 1996. Cardiacα-adrenergic receptor expression is regulated by thyroid hormone during a critical developmental period. J. Mol. Cell. Cardiol. 28 (5), 1033–1044.
Miura, K., Mineta, H., 2014. Histological evaluation of thyroid lesions using a scanning acoustic microscope. Pathol. Lab. Med. Int. 2014 (6), 1–9.
Noyes, P.D., Lema, S.C., Macaulay, L.J., Douglas, N.K., Stapleton, H.M., 2013. Low level exposure to the flame retardant BDE-209 reduces thyroid hormone levels and disrupts thyroid signaling in fathead minnows. Environ. Sci. Technol. 47 (17), 10012–10021.
Pawlikowski, M., Jaranowska, M., Pisarek, H., Kubiak, R., Fuss-Chmielewska, J., Winczyk, K., 2015. Ectopic expression of follicle-stimulating hormone receptors in thyroid tumors. Arch. Med. Sci. 11 (6), 1314–1317.
Qiao, L., Zheng, X.B., Yan, X., Wang, M.H., Zheng, J., Chen, S.J., Yang, Z.Y., Mai, B.X., 2018. Brominated flame retardant (BFRs) and Dechlorane Plus (DP) in paired human serum and segmented hair. Ecotoxicol. Environ. Saf. 147, 803–808.
Rahman, F., Langford, K.H., Scrimshaw, M.D., Lester, J.N., 2001. Polybrominated diphenyl ether (PBDE) flame retardants. Sci. Total Environ. 275 (1–3), 1–17.
Richardson, V.M., Staskal, D.F., Ross, D.G., Diliberto, J.J., DeVito, M.J., Birnbaum, L.S., 2008. Possible mechanisms of thyroid hormone disruption in mice by BDE 47, a major polybrominated diphenyl ether congener. Toxicol. Appl. Pharmacol. 226 (3), 244–250.
Sabino, M., Capomaccio, S., Cappelli, K., Verini-Supplizi, A., Bomba, L., Ajmone-Marsan, P., Cobellis, G., Olivieri, O., Pieramati, C., Trabalza-Marinucci, M., 2018. Oregano dietary supplementation modifies the liver transcriptome profile in broilers: RNASeq analysis. Res. Vet. Sci. 117, 85–91.
Salabè, G.B., 2001. Pathogenesis of thyroid nodules: histological classification? Biomed. Pharmacother. 55 (1), 39–53.
Segaloff, D.L., Ascoli, M., 2013. Thyroid-stimulating hormone/luteinizing hormone/follicle-stimulating hormone receptors. Encycl. Biol. Chem. 387–391.
Sun, S., Jin, Y., Yang, J., Zhao, Z., Rao, Q., 2021. Nephrotoxicity and possible mechanisms of decabrominated diphenyl ethers (BDE-209) exposure to kidney in broilers. Ecotoxicol. Environ. Saf. 208 (2021), 111638.
Szkudlinski, M.W., Fremont, V., Ronin, C., Weintraub, B.D., 2002. Thyroid-stimulating hormone and thyroid-stimulating hormone receptor structure-function relationships. Physiol. Rev. 82 (2), 473–502.
Tebourbi, O., Hallègue, D., Yacoubi, M.T., Sakly, M., Rhouma, K.B., 2010. Subacute toxicity of p, p′-DDT on rat thyroid: Hormonal and histopathological changes. Environ. Toxicol. Pharmacol. 29 (3), 271–279.
Trapnell, C., Williams, B.A., Pertea, G., Mortazavi, A., Kwan, G., van Baren, M.J., Salzberg, S.L., Wold, B.J., Pachter, L., 2010. Transcript assembly and quantification by RNA-Seq reveals unannotated transcripts and isoform switching during cell differentiation. Nat. Biotechnol. 28 (5), 511–515.
Turyk, M.E., Persky, V.W., Imm, P., Knobeloch, L., Chatterton, R., Anderson, H.A., 2008. Hormone disruption by PBDEs in adult male sport fish consumers. Environ. Health Perspect. 116 (12), 1635–1641.
Wang, Y., Chen, T., Sun, Y., Zhao, X., Zheng, D., Jing, L., Zhou, X., Sun, Z., Shi, Z., 2019. A comparison of the thyroid disruption induced by decabrominated diphenyl ethers (BDE-209) and decabromodiphenyl ethane (DBDPE) in rats. Ecotoxicol. Environ. Saf. 174, 224–235.
Wei, J., Liu, J., Liang, S., Sun, M., Duan, J., 2020. Low-dose exposure of silica nanoparticles induces neurotoxicity via neuroactive ligand–receptor interaction signaling pathway in zebrafish embryos. Int. J. Nanomed. 15, 4407–4415.
Wilford, B.H., Shoeib, M., Harner, T., Zhu, J., Jones, K.C., 2005. Polybrominated diphenyl ethers in indoor dust in Ottawa, Canada: implications for sources and exposure. Environ. Sci. Technol. 39 (18), 7027–7035.
Woyengo, T.A., Bogota, K.J., Noll, S.L., Wilson, J., 2018. Enhancing nutrient utilization of broiler chickens through supplemental enzymes. Poult. Sci. 98 (3), 1302–1309.
Yu, G., Bu, Q., Cao, Z., Du, X., Xia, J., Wu, M., Huang, J., 2016. Brominated flame retardants (BFRs): a review on environmental contamination in China. Chemosphere 150, 479–490.
Zhu, N.Z., Liu, L.Y., Ma, W.L., Li, W.L., Song, W.W., Qi, H., Li, Y.F., 2015. Polybrominated diphenyl ethers (PBDEs) in the indoor dust in China: levels, spatial distribution and human exposure. Ecotoxicol. Environ. Saf. 111, 1–8.
Zoeller, R.T., Tan, S.W., Tyl, R.W., 2007. General background on the hypothalamic-pituitary-thyroid (HPT) axis. Crit. Rev. Toxicol. 37 (1–2), 11–53.